

# Proximity Based Object Segmentation in Natural Color Images Using the Level Set Method

Nguyen Tran Lan Anh<sup>†</sup>, *Nonmember*, and Guesang Lee<sup>†(a)</sup>, *Member*.

**SUMMARY** Segmenting indicated objects from natural color images remains a challenging problem for researches of image processing. In this paper, a novel level set approach is presented, to address this issue. In this segmentation algorithm, a contour that lies inside a particular region of the concerned object is first initialized by a user. The level set model is then applied, to extract the object of arbitrary shape and size containing this initial region. Constrained on the position of the initial contour, our proposed framework combines two particular energy terms, namely local and global energy, in its energy functional, to control movement of the contour toward object boundaries. These energy terms are mainly based on graph partitioning active contour models and Bhattacharyya flow, respectively. Its flow describes dissimilarities, measuring correlative relationships between the region of interest and surroundings. The experimental results obtained from our image collection show that the suggested method yields accurate and good performance, or better than a number of segmentation algorithms, when applied to various natural images.

**Keywords:** *object-of-interest segmentation; Bhattacharyya flow; graph partitioning; level set; natural color image.*

## 1. Introduction

Image segmentation plays an important role in image processing and computer vision. This step helps to provide valuable information of images in the simplest way. A remarkable growth in the number of color object segmentation algorithms has taken place. But it is a hard task, due to real-world variations in color distribution, object category, position, and size, among others. Recently, variational methods have been extensively studied for the scope of segmentation, because of their flexibility in modeling, and advantages in numerical implementation. When the aim is to detect all salient objects, level set methods are very efficient. However, if users would like to segment only “one object” of interest at a specified location, as well as remove surrounding similar characteristic regions in the image, segmentation using level set approaches becomes worse. An example of limitations of the model is illustrated in Fig. 1.

To start this study, there are two constraints on the applicable images and objects. The first constraint is

“one object”, indicating a single object or a group of objects that not only have similar properties (e.g. colors, texture, etc.), but are also stuck together, as shown in Fig. 2. The second constraint is “proximity”. Although color is normally used as a main clue to identify an object, it is not enough to satisfy our specific problem. There can be objects that have the same color, but are in different locations. For this reason, proximity information provided by user interaction, or a small circle inside the object of interest, should be embedded. Thus we call our proposed model the ‘proximity-based level set’ method.

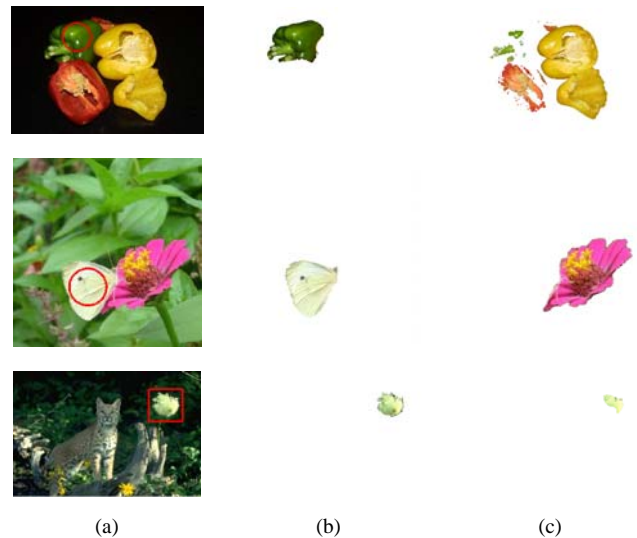


**Fig. 1.** Limitations of level set methods for segmenting a single object of interest, (a): color images with user-initialized contour, (b): desired results, and (c): wrong segmentation results

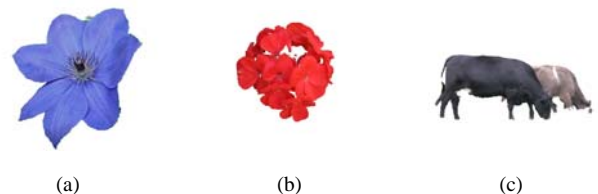


**Fig. 2.** Illustrations of the definition of the term “one object”, (a): “One object” is a single flower, (b): “One object” is a bunch of red small flowers, and (c): This case is not considered as “one object”

The aim of our model is to use proximity information, to keep the contour moving around the location where it is initialized manually by users, and segment only “one object” containing this region.

Manuscript received January xx, 20xx.

Manuscript revised March xx, 20xx.

<sup>†</sup>The authors are with the Department of Electronics and Computer Engineering, Chonnam National University, Republic of Korea. a) Corresponding author: gslee@jnu.ac.kr

Compared to other works, our contribution is to modify the original energy functional in the level set method. Two different energy terms, inspired by individual advantages of both the Bhattacharyya flow and the graph partitioning active contour (GPAC), are combined, and a new distance relationship measured between any two pixels is added. This information helps constrain our model to segment only one object of interest, in the location where the contour is initialized manually by the user. In this approach, objects can consist of various color or texture parts, whose differences should be small enough. If their color differences are highly inhomogeneous with the color of the interested region, or the details inside textures are highly different, these parts will be considered to not belong to the object of interest.

The remainder of this paper is organized as follows. Some related works are reviewed in Section 2. Our method and experimental results are discussed in Sections 3 and 4, respectively. Finally, Section 5 gives our conclusions.

## 2. Related Works

In general, many works have extensively reported about image segmentation. These all rely on a wide range of strategies, such as statistics, differential geometry, heuristics, graph theory and algebra. Moreover, they can act automatically, by taking no user input, or interactively, by using user hints for initialization or guidance. Traversing the huge amount of existing techniques, they can be categorized into four types of segmentation: thresholding, boundary-based, region-based, and hybrid algorithms. Among them, thresholding algorithms assume that clusters in the histogram correspond to either background or foreground, and can be extracted by separating these clusters [1, 2]. Boundary-based methods assume that the pixel properties change abruptly between different regions [3, 4]. From a different viewpoint, region-based methods assume that neighboring pixels within the same region should have similar values [5, 6]. Both pixel and region properties in these two types can be either the intensity (mostly in gray-scale images), color (in color images), or texture information, and be attached as a feature vector to each pixel or region. Commonly, a new segmentation algorithm usually starts as gray-level segmentation, and later develops to handle color and textured images. The most advanced methods today are hybrid models, which tend to combine both above attitudes, boundary detection and region growing, to generally achieve the best results [7, 8].

In particular, for better segmenting dynamic-shape objects in medical images, the active contour model (ACM) was first introduced by Kass, Witkins, and Terzopoulos [9] in 1987, as an interactive segmentation model for 2D images. It is also called the snake or

deformable model. Those methods start with a contour drawn by the user, and iteratively deform it under an energy minimization framework, to get the final, best describing object contour. To minimize this energy, both external forces and internal forces are used, to attract the contour to its right place, and to keep the contour smooth, respectively. Various external constraints, such as the gradient or gradient vector flow of the image, are embedded in a speed function [10-13]. Snake models have been applied to many applications, despite a few problems associated with their initialization, and poor convergence to boundary concavities. Subsequently, Osher and Sethian [14] first proposed the level set method in fluid dynamics in 1988. Its basic idea is to embed a 2D contour in a surface in 3D. Applying it to image segmentation was suggested by Malladi and Sethian [15]. An active contour is described as the zero level set of a level set function (LSF) for controlling the evolution of the curve, rather than only tracking the boundaries of objects.

According to the nature of color images, it is remarkable to inherit strong points of various existing ACMs with different information cues, to lead to a powerful segmentation algorithm. The Geodesic-Aided Chan-Vese (GACV) method [16] is a typical example. One more example is the color-texture image segmentation by augmenting region and photometric invariant edge information model [17]. Another important proposed ACM is the distance regularized level set evolution algorithm [18, 19], for eliminating the need for a costly re-initialization procedure, if the initial contour is a signed distance function. Because of its effectiveness, this distance regularization term has then come into widespread use in many energy functionals, to help ACMs perform better [20, 21]. For ever-growing research, combinations of ACMs and other segmentation methods gave new ideas, and opened up incredible progress to solve this problem. These can be stochastic representations [22, 23], graph partitioning methods [24, 25], generic algorithms [26], etc. used to define variational cost functions. Among these models, graph partitioning active contour (GPAC) proposed by Sumengen and Manjunath in 2006 [27] is nearly closest to the underlying framework of the C-V model, by its global minimization techniques. Its concept is based on the minimum-cut formulation, to reformulate the problem in a continuous domain, and solve it using active contour in the level set framework, rather than graph-cuts. Hence, an improvement of a GPAC model could be considered for our particular problem, to suit our requirements, increasing its performance related to convergence speed and accuracy, as well as letting the contour be smoother.

### 3. Proximity Based Object Segmentation Using the Level Set Method

#### 3.1 System Overview

A flowchart of the proposed method is depicted in **Fig. 3**. First, we construct a graph, by taking each pixel of the input image as a node, and define a dissimilarity value between any two nodes as an edge weight. A process of finding a bounding contour is repeated, to achieve the segmentation of the object we concerned. In this process, the energy functional of the proposed level set method is updated iteratively. The number of pixels whose energy value changes its sign is then counted, and compared with a threshold number. If this stopping condition is not satisfied, the process will continue, by updating the dissimilarity value of each pair of nodes in the graph. Otherwise, the object of interest is segmented.

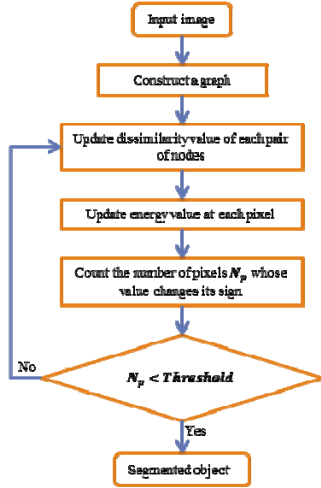


Fig. 3. Proposed method flowchart

#### 3.2 Graph Partitioning Active Contour

In Ref. [27], Sumengen and Manjunath introduced a new curve evolution framework to ACMs, called Graph Partitioning Active Contours (GPAC). This framework is motivated by the relationship between active contours and graph theoretic methods. Their combination is based on pairwise similarities between points on the curve  $C$ , or dissimilarities of across-region cuts. In a continuous domain, in order to maximize the dissimilarities between regions, a variational cost function of curve evolution based on minimum cut criterion for pairwise similarities can be formulated as

$$E_{CR}(C) = \iint_{R_i(C)} \iint_{R_o(C)} \omega(u, v) dudv \quad (1)$$

where,  $R_i(C)$  and  $R_o(C)$  are the interior and exterior regions of  $C$ ,  $u$  and  $v$  are points such that  $u \in R_i$ ,  $v \in R_o$ , and  $\omega(u, v)$  is a similarity measure between points  $u$  and

$v$ . Double integrals reflect the integration over a 2D region. Minimization of  $E_{CR}(C)$  with respect to the curve  $C$  results in partitioning of the image, which minimizes the similarity between regions  $R_i(C)$  and  $R_o(C)$ . Using the steepest descent method, where a curve is instantiated and evolved toward the expected minimum, the problem will be solved.

Without any loss of generality,  $\omega(u, v)$  can be a dissimilarity metric. At that time, the cost function should be maximized, as opposed to the above minimization, by

$$E_{CR}(C) = - \iint_{R_i(C)} \iint_{R_o(C)} \omega(u, v) dudv \quad (2)$$

To measure the dissimilarity metric in Eq. 2,  $L_1$ ,  $L_2$  and  $L_p$ -norms can be used on color features. But in general cases, GPAC can use more complex dissimilarity measures that integrate spatial distance of pixels and domain knowledge. In Ref. [28], Bertelli et al. reformulated the above across-region cut from Ref. [29], in terms of pairwise dissimilarity within each region. Its objective is to minimize the intra-region dissimilarity by

$$E_{WR}(C) = \iint_{R_i(C)} \iint_{R_i(C)} \omega(u, v) dudv + \iint_{R_o(C)} \iint_{R_o(C)} \omega(u, v) dudv \quad (3)$$

Actually, there are many advantages of using this GPAC in object segmentation problems [27]. One of them is that some geometric properties or constraints can be introduced into the curve evolution equation, without changing or resolving the energy minimization problem, due to the use of geometric ACM. Secondly, the theory developed in this variational framework can be easily adapted, and applied to other cost functions that are based on pairwise (dis)similarities. Furthermore, GPAC is a region-based model for segmentation; but it can offer a flexible framework where edge information can be integrated, to help extract more precise boundaries. Since then, a lot of modifications can be flexibly considered for GPAC, to increase its performance the most.

#### 3.3 The Bhattacharyya Flow

A number of measures can be used to compute a distance between probability distributions, including the Fisher ratio, Kullback-Leibler divergence, Bhattacharyya distance, and Hellinger distance. Among these measures, the Bhattacharyya distance is invariant to transformations on feature space [30], with relatively simple analytical form [31].

The Bhattacharyya distance [30] formally gives a measure of similarity between two probability distributions, defined as  $D = -\log B$ , where  $B$  is the Bhattacharyya coefficient

$$B = \int_Z \sqrt{P_{in}(z) P_{out}(z)} dz \quad (4)$$

In the image processing field,  $z \in Z$  is a photometric variable, such as the intensity, a color vector, or a texture vector, and lives in  $Z$ , the space of the photometric variable.  $P_{in}$  and  $P_{out}$  are probability distributions defined on the variable  $z$  for the inside and outside regions, respectively. It is noted that maximizing the Bhattacharyya distance  $D$  is equivalent to minimizing  $B$ . This measure varies between 0 and 1, where 0 indicates a complete mismatch, and 1 indicates complete agreement between the probability distributions. Equivalently, the final contour in ACMs is obtained when the overlap between the intensity distributions of object and background (inside and outside the contour) is minimized.

Let  $x \in \mathcal{R}^2$  specify the coordinates in the image plane, and  $I : \Omega \subset \mathcal{R}^2 \rightarrow Z$  be a mapping from the image plane to the space of the photometric variable. For the case of curve evolution, the probability distribution  $P_{in}$  (or  $P_{out}$ ) is assumed to be defined by the density of the region inside the curve  $C$ . Thus, in terms of the level set function  $\phi$ , we get

$$P_{in}(z) = \frac{\int_{\Omega} K(z-I(x))H(-\phi(x))dx}{\int_{\Omega} H(-\phi(x))dx} \quad (5)$$

where,  $H$  is the Heaviside step function, and  $\Omega$  is the whole image domain. Similarly,  $P_{out}$  can be rewritten as

$$P_{out}(z) = \frac{\int_{\Omega} K(z-I(x))H(\phi(x))dx}{\int_{\Omega} H(\phi(x))dx} \quad (6)$$

Computing the first variation of Eq. 4, we get the following

$$\begin{aligned} \frac{\partial P_{in}(z)}{\partial \phi} &= \frac{\delta_{\varepsilon}(\phi)}{A_{in}} (P_{in}(z) - K(z-I(x))) \\ \frac{\partial P_{out}(z)}{\partial \phi} &= \frac{\delta_{\varepsilon}(\phi)}{A_{out}} (K(z-I(x)) - P_{out}(z)) \end{aligned} \quad (7)$$

$$\nabla_{\phi} B = \frac{1}{2} \int_Z (P_{in}(z)P_{out}(z))^{-1/2} \times \left( \frac{\partial P_{in}(z)}{\partial \phi} P_{out}(z) + \frac{\partial P_{out}(z)}{\partial \phi} P_{in}(z) \right) dz$$

where,  $\delta_{\varepsilon}(\phi)$  is a smooth approximation of the Dirac delta function, and  $A_{in}$  and  $A_{out}$  is the area inside and outside the curve, respectively. Combining all of the equations above, we obtain the following PDE:

$$\begin{aligned} \frac{\partial \phi(x,t)}{\partial t} &= -\frac{B\delta_{\varepsilon}(\phi)}{2} \left( \frac{1}{A_{in}} - \frac{1}{A_{out}} \right) \\ &\quad - \frac{\delta_{\varepsilon}(\phi)}{2} \times \int_Z K(z-I(x)) \left( \frac{1}{A_{out}} \sqrt{\frac{P_{in}(z)}{P_{out}(z)}} - \frac{1}{A_{in}} \sqrt{\frac{P_{out}(z)}{P_{in}(z)}} \right) dz \end{aligned} \quad (8)$$

The first term in this equation determines the ‘‘global’’ direction in which the entire curve moves, whereas the second term determines the ‘‘local’’ evolution direction. Thus, the initial motion of the curve is minimal when  $B$  is close to zero, indicating convergence of the curve evolution.

### 3.4 Proximity Based Object Segmentation Using the Level Set Method

Generally, a level set method is commonly defined by a particular energy functional describing features of the object we want to segment. So, the energy functional in our proposed algorithm includes two primary elements: a local energy based on GPAC, and a global energy based on the Bhattacharyya flow.

In this work, for the local energy term, our basic variational cost oppositely relies on the within region dissimilarity shown in Eq. 3, and the evolution of the front  $C$  is done implicitly, using the level set framework. Therefore, the local energy term takes into account the dissimilarity within each segment.

For the global energy term, the Bhattacharyya flow helps measure the overlap between the intensity distributions of the background and foreground regions. Consequently, not only the differences within each region are minimized, but the distance between the two regions is maximized as well. Essentially, our fitting energy functional is written as the following

$$E(C) = \sigma E_{local}(C) + (1-\sigma) E_{global}(C) \quad (9)$$

where,  $\sigma$  is the balance coefficient  $0 \leq \sigma \leq 1$  to control the effect of the local and global terms,  $E_{local}(C) = E_{WR}(C)$ , and  $E_{global}(C) = E_{Bha}(C)$ . To be suited to the nature of color images, the dissimilarity measure in Eq. 3 for calculating  $E_{local}(C)$  uses  $L_2$  distance on color and location features, as below:

$$\begin{aligned} \omega(u,v) &= \frac{\|I(u)-I(v)\|}{\sqrt{3}} \\ &\quad + \frac{1}{l_{diag}^2} \times \begin{cases} 0 & u,v \in RIC \\ \text{dist}(u,RIC) & u \notin RIC, v \in RIC \\ \text{dist}(v,RIC) & u \in RIC, v \notin RIC \\ \text{dist}(u,RIC)\text{dist}(v,RIC) & u \notin RIC, v \notin RIC \end{cases} \end{aligned} \quad (10)$$

where, RIC is the abbreviation of the ‘‘region inside the curve’’,  $l_{diag}^2$  is the square of the length of the diagonal of the image, and  $\text{dist}(u,RIC) = \min \text{dist}(u,x)$  for all points  $x \in \partial C$ .  $I(u)$  is a vector of the three channels, namely the red, green, and blue color components of pixel  $u$  and each channel  $I^i(u) \in [0,1]$ , so  $\|I(u)-I(v)\| \in [0, \sqrt{3}]$ . The Bhattacharyya coefficient is rewritten as the summation of  $B$  values, computed from both three-color channels:

$$E_{Bha}(C) = \sum_{i=1}^3 B^i(C) \quad (11)$$

While the cost function presented above demonstrates a great potential for image segmentation, its usefulness has been limited. The problem is that the contributions of within region dissimilarity of different regions (i.e. inside

and outside the curve) in the level set formulation are the same. This can compound the slowness of contours evolution (or iterative speed), and the sharpness of the contours. To overcome these weaknesses, a condition is supposed, in which different regions have different contribution to the energy functional. We alleviate it by using the image entropy, to add coefficients to two elements of the traditional energy functional. At the same time, based on the advantages of GPAC mentioned in section 3.2, we can add normalization for the integrals in Eq. 3, by dividing them with their corresponding areas. The main reason for this is that the cuts usually favor equal size regions. For images where the foreground is larger or smaller than the background, it is more efficient to use normalized cuts. Thus, the energy function is rewritten as follows

$$E_{local}(C) = \frac{E_{in}}{A_{in}} \iint_{R_i(C)} \iint_{R_i(C)} \omega(u,v) dudv + \frac{E_{out}}{A_{out}} \iint_{R_o(C)} \iint_{R_o(C)} \omega(u,v) dudv \quad (12)$$

As in most level set methods, we need to smooth the contour  $C$  during evolution, by penalizing its length, called  $Length(C)$ . Finally, in our own approach, the energy functional is introduced as the following

$$E(C) = \nu Length(C) + \sigma E_{local}(C) + (1-\sigma) E_{global}(C) \quad (13)$$

where,  $\nu > 0$  is a constant as the weight of the length term. Minimizing the proposed energy function, we can find a contour  $C$ , such that the below goals could be achieved:

- The length term is minimized;
- the image is partitioned into two regions (inside and outside the curve  $C$ ), such that the dissimilarity within each region is minimized; and
- the Bhattacharyya distance between these two regions is maximized.

To deal with topological changes, we transform this energy functional into the level set formulation. In addition, to penalize the deviation of the LSF  $\phi$  from a SDF, a distance regularization term, based on a double-well potential function, is added to our proposed energy functional. Lastly, minimization of the energy function in Eq. 13 with respect to  $\phi$  is used to derive the evolution flow equation, as follows:

$$\begin{aligned} \frac{\partial \phi}{\partial t} = & \delta_z(\phi) \left\{ \nu \text{div} \left( \frac{\nabla \phi}{|\nabla \phi|} \right) \right. \\ & - \sigma \left( \frac{E_{in}}{A_{in}} \iint_{R_i} \alpha(u,v) dudv + \frac{E_{out}}{A_{out}} \iint_{R_o} \alpha(u,v) dudv \right) \\ & \left. - (1-\sigma) \sum_{i=1}^3 \left[ \frac{B^i}{2} \left( \frac{1}{A_{in}} - \frac{1}{A_{out}} \right) + \frac{1}{2} \int_Z \delta(z-I^i) \left( \frac{1}{A_{in}} \sqrt{\frac{P_{in}^i}{P_{out}^i}} - \frac{1}{A_{out}} \sqrt{\frac{P_{out}^i}{P_{in}^i}} \right) dz \right] \right\} \\ & + \mu \text{div} \left( d_p(|\nabla \phi|) \nabla \phi \right) \end{aligned} \quad (14)$$

where,  $\delta_\varepsilon(\phi)$  is the smooth approximation of the Dirac delta function,  $\mu$  is a constant controlling the deviation of  $\phi$  during its propagation,  $\text{div}(\bullet)$  is the divergence operator, and  $d_p$  is a function defined by

$$d_p(s) = \frac{p'(s)}{s} \quad (15)$$

and  $A_{in}$  and  $A_{out}$  are given by

$$A_{in} = \int_{\Omega} H(-\phi(x)) dx, \quad A_{out} = \int_{\Omega} H(\phi(x)) dx \quad (16)$$

In Eq. 15, we use a specific construction of the double-well potential  $p_2(s)$ , described in Refs. [18, 19] as:

$$p_2(s) = \begin{cases} \frac{1}{(2\pi)^2} (1 - \cos(2\pi s)) & \text{if } s \leq 1 \\ \frac{1}{2} (s-1)^2 & \text{if } s \geq 1 \end{cases} \quad (17)$$

Note that in digital images, the two probability distributions  $P_{in}^i$  and  $P_{out}^i$  in Eq. 14 are simply the histograms inside and outside the curve in the  $i^{\text{th}}$  color channel of the image.

At each iteration,  $\phi$  is updated. Not considering  $\phi$  in a whole image, our algorithm only focuses on pixels whose values change in sign. At that time, a checking condition is suggested, to identify its probability of belonging to the current desired object. If the shortest distance between this pixel and the previous zero level set contour satisfies a threshold, it will be considered to be within the a priori known size of the width of contour neighborhood. Thus, only sign-changed pixels within the contour neighborhood are replaced by its new value, until the object of interest is completely achieved. Other surrounding objects, which are far away but have color similarity, are easily eliminated, if the contour is split, and attracted to their locations, as a characteristic of the level set framework.

#### 4. Experimental Results

For all experiments in this work, the proposed method was implemented in MATLAB version 7.12.0 (R2011a). Some functions related to GPAC code by Luca Bertelli [28] written by C++ programming language and compiled as the *mex* files are also used. This program runs on a PC equipped with an Intel® Core™2 CPU 6700 at 2.66 GHz, 2.67 GHz and 2 GB of RAM. Parameter values in Eq. 14 are set as  $\varepsilon = 0.001$ ,  $\nu = 4000$ ,  $\sigma = 0.5$ ,  $\mu = 0.04$ , and the time step as  $\Delta t = 0.5$ . Convergence is achieved if the number of sign-changed energy value of pixels is smaller than a threshold of 20 pixels, in this work.

We evaluated the performance of the proposed algorithm on 104 natural color images. The image database used here is collected from a variation of the publicly available datasets provided by Achanta et al. [31], Berkeley Segmentation Dataset (BSDS500) [32], and Microsoft Research Cambridge (MSRC) [33, 34], to suit our specific problem. These color images can contain one or many single objects, which have similar or dissimilar properties (i.e. colors, texture, etc.). Because of the complexity of the algorithm, all images are reduced in size to be smaller than 400 pixels in each dimension (height and width). There are a total of 136 objects in these images. The final results are then compared with their ground truth by quantitative metrics i.e. average precision, recall and F-Measure, defined as follows

$$F\text{-measure} = (1 + \beta^2) \frac{\text{Precision} \times \text{Recall}}{\beta^2 \times \text{Precision} + \text{Recall}} \quad (18)$$

The relative weight between the precision and recall controlled by  $\beta^2$  is set to 0.5. By giving this weight value to these metrics, we put more emphasis on precision, than recall.

**Fig. 4** visualizes the evolution of our proposed segmentation algorithm applied to a  $400 \times 266$  color image. The original image is **Fig. 4 (a)**, in which we look forward to segment the biggest yellow flower. It is depicted accurately in **Fig. 4 (c)**. The initial zero level set is shown by a green circle, given by the user, in **Fig. 4 (b)**. Starting from this region, **Figs. 4 (d), (e), and (f)** are, in turn, results obtained at the 5th, 14th, and final (or 59th) step of the propagation, respectively. It takes approximately 17 seconds in total. The final contour looks quite smooth, and almost fits the object of interest. In particular, the algorithm can separate our considered flower from the neighboring one, due to the distance constraint added to the dissimilarity measure in Eq. 10.

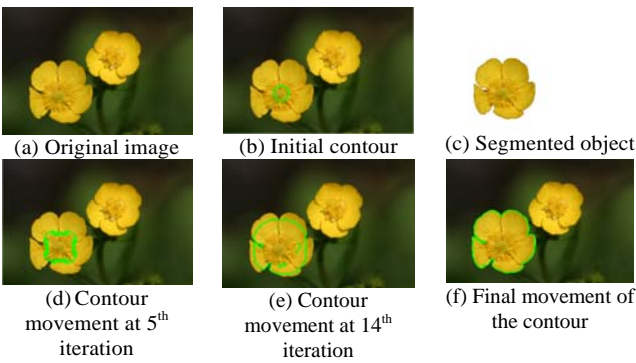


**Fig. 4.** Object of interest segmentation process, by our proximity-based level set method

The next figure illustrates a visual comparison between the output of our proposed method, and six different segmentation methods with different user interactive initializations. These algorithms include the marker-based watershed [35], GrabCut [36], fixation-

based active segmentation [37], Graph partitioning active contour (GPAC) [27], RGAC model [38], and Chan-Vese model for vector-valued images [39]. In this figure, **Figs. 5 (c), (d), (e), and (f)** are initializations for fixation-based active segmentation, GrabCut, marker-based watershed, and all remaining models, respectively. Corresponding to the initializations in **Figs. 5 (c), (d), and (e)**, the segmentation results are given in **Figs. 5 (g), (h), and (k)**, respectively. Finally, **Figs. 5 (l), (m), (n), (o)** are results of objects segmented from the initial green circle in **Fig. 5 (f)**. As shown in **Fig. 5**, our location-based ACM gives the most exact segmentation in comparison with its ground truth image, when compared with the other methods.

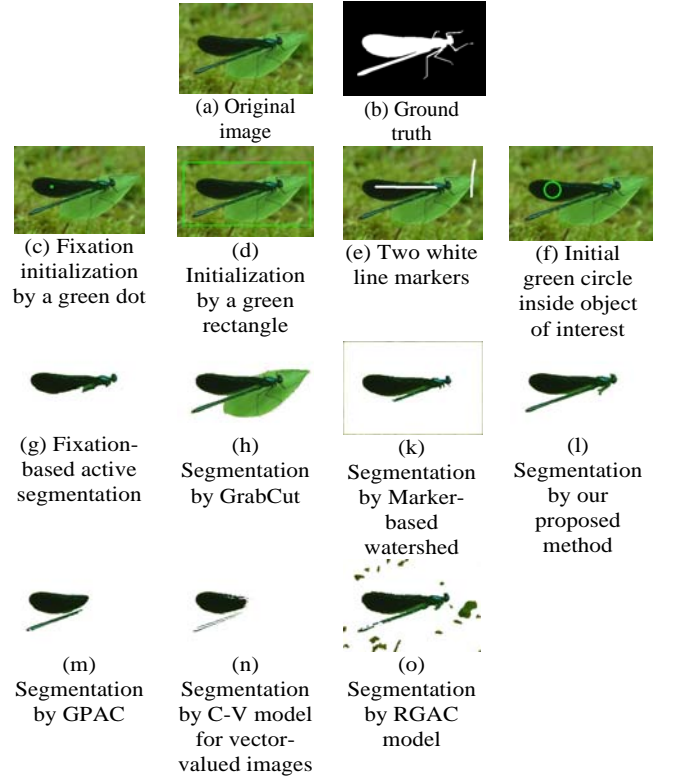


**Fig. 5.** Some object of interest segmentation results

**Table 1.** Comparison of user interactive segmentation methods.

Method	Precision	Recall	F-measure
Marker-based watershed	0.66	0.84	0.73
GrabCut	0.79	0.84	0.80
Fixation-based active segmentation	0.94	0.72	0.75
GPAC	0.79	0.78	0.75
RGAC	0.50	0.77	0.60
C-V model for vector-valued image	0.58	0.58	0.59
<b>Our proposed method</b>	<b>0.86</b>	<b>0.82</b>	<b>0.81</b>

**Table 1** summarizes the performance of various segmentation methods applied to our entire image database. The results show that the proposed method can successfully segment only “one object” of interest in

various natural images with a lower false-positive rate or a higher precision, compared to the other level set-based methods. Since the other level set-based ACMs in the comparison do not consider the proximity relationship between pixels and the initial region, they are very sensitive to colors, and therefore produce many false positives. Compared to different user interactive algorithms, our proposed method generally achieves good performance, as well.

Based on our definition of “one object”, there are some special cases considered intensively in **Figs. 6** and **7**. If there is a single object in the image, our proposed model can work effectively. Otherwise, **Fig. 6** represents illustrations of the appearance of many single objects in the image. There are the three following cases:

- Single objects are separate from each other, and their colors are almost the same (see **Fig. 6 (a)**).
- Single objects are stuck together, and their colors are almost the same (see **Fig. 6 (b)**).
- Single objects are stuck together, and their colors are quite different (see **Fig. 6 (c)**).

In the first case, our proposed method can segment the object selected by user-initialized contour (see **Fig. 6 (d)**) successfully. In the second case, however, these two horses have to be considered as “one object”. At that time, our model will segment both of them out of the background (see **Fig. 6 (e)**). This is one of our limitations, when the proposed algorithm cannot distinguish them as two distinct horses. The good segmentation result of the final case is shown clearly in **Fig. 6 (f)**.

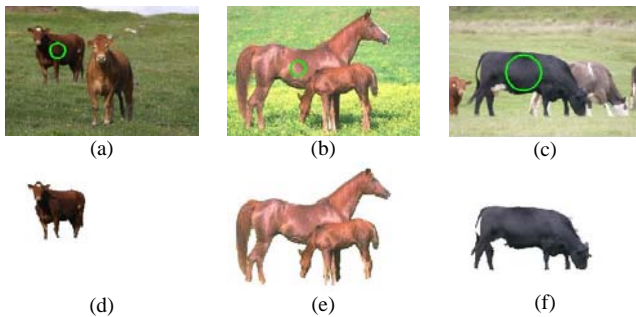


**Fig. 6** Segmentation results of single objects appearing in images

Another special case shown in **Fig. 7** belongs to objects that are sometimes partially hidden behind something. For example, **Fig. 7 (a)** shows a leaf partially hidden behind a reptile. Our target is to segment this leaf out of the image. After running iteratively, our proposed method can not only extract it but also reject the reptile inside it completely (see **Fig. 7 (b)**). However, in **Fig. 7 (c)**, a branch of a tree hides a part of a bird, as well as splitting the bird into two separate parts. In this case, our suggested model can segment only one among these parts. This is another of our limitations, due to its constraint on proximity information (see **Fig. 7 (d)**).

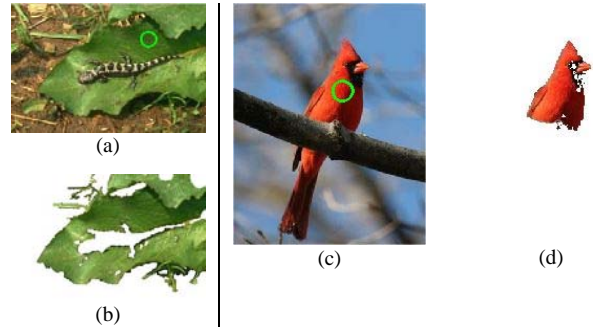


**Fig. 7** Segmentation of objects that are partially hidden behind something

## 5. Conclusions

In this paper, a proximity based level set method to deal with segmenting “one object” of interest in color images has been presented. A combination of global and local energy terms within the energy functional is employed, to deform the initial contour towards boundaries of the object, as well as guarantee its convergence after a finite number of iterations. The experimental results show that our suggested method generates promising results on various natural images. The comparison with six different segmentation methods also proves that our approach is robust, and mostly satisfies the problem. However, there are some limitations, where our proposed ACM fails. In the future we will try to optimize and improve our method for segmenting more accurately, for special cases, as well as advanced tasks.

## Acknowledgement

This research was supported by Basic Science Research Program through the National Research Foundation of Korea(NRF) funded by the Ministry of Education, Science and Technologies(2012-047759) and the MKE (The Ministry of Knowledge Economy), Korea, under the ITRC (Information Technology Research Center) support program supervised by the NIPA (National IT Industry Promotion Agency) (NIPA-2013-H0301-13-3005).

## References

- [1] H.D. Cheng, C.H. Chen, H.H. Chiu, and H. Xu, “Fuzzy homogeneity approach to multilevel thresholding,” *IEEE Transactions on Image Processing*, Vol. 7, pp. 1084-1086, 1998.
- [2] H.D. Cheng, X.H. Jiang, and J. Wang, “Color image segmentation based on homogram thresholding and region merging,” *Pattern Recognition*, Vol. 35, pp. 373-393, 2002.
- [3] J. Basak and B. Chanda, “On edge and line linking with connectionist model,” *IEEE Transactions on System, Man, and Cybernetics*, Vol. 24, pp. 413-428, 1994.
- [4] F.Y. Shih and S. Cheng, “Adaptive mathematical morphology for edge linking,” *Information Sciences*, Vol. 167, pp. 9-21, 2004.
- [5] S.A. Hojjatoleslami and J. Kittler, “Region growing: a new

- approach," *IEEE Transactions on Image Processing*, Vol. 7, pp. 1079-1084, 1998.
- [6] N. Ikonomakis, K.N. Plataniotis, M. Zervakis, and A.N. Venetsanopoulos, "Region growing and region merging image segmentation" *Proceedings of IEEE Conference on Digital Signal Processing*, Vol. 1, pp. 299-302, 1997.
- [7] Y. Deng and B.S. Manjunath, "Unsupervised segmentation of color-texture regions in images and video," *IEEE Transactions of Patter Analysis and Machine Intelligence*, Vol. 23, pp. 800-810, 2001.
- [8] J. Fan, D.K.Y. Yau, A.K. Elmagarmid, and W.G. Aref, "Automatic image segmentation by integrating color-edge extraction and seeded region growing," *IEEE Transactions on Image Processing*, Vol. 10, pp. 1454-1466, 2001.
- [9] M. Kass, A. Witkin, and D. Terzopoulos, "Snakes: Active contour models," *International Journal of Computer Vision*, Vol. 1, pp. 321-331, 1987.
- [10] V. Caselles, R. Kimmel, and G. Sapiro, "Geodesic active contours," *Proc. IEEE Fifth International Conference on Computer Vision*, pp. 694-699, 1995.
- [11] C. Xu and J.L. Prince, "Gradient vector flow: A new external force for snakes," *IEEE Proceedings of Conference on Computer Vision and Pattern Recognition*, pp. 66-71, 1997.
- [12] S. Osher and R. Fedkiw, *Level set methods and Dynamic implicit surface*, Springer, New York, 2003.
- [13] J.A. Sethian, *Level set methods and Fast marching methods*, Cambridge University Press, Cambridge, 1999.
- [14] S. Osher and J. Sethian, "Fronts propagating with curvature-dependent speed: Algorithms based on Hamilton-Jacobi formulations," *Journal of Computational Physics*, Vol. 79, pp. 12-49, 1988.
- [15] R. Malladi, J.A. Sethian, and B.C. Vemuri, "Shape modeling with front propagation: A level set approach," *IEEE Trans. Pattern Anal. Mach. Intelligence*, Vol. 17(2), pp. 158-175, 1995.
- [16] L. Chen, Y. Zhou, Y. Wang, and J. Yang, "GACV: Geodesic-Aided C-V Method," *Pattern Recognition*, Vol. 39, pp. 1391-1395, 2006.
- [17] Z. Ying, L. Guanyao, S. Xiehua, and Z. Xinmin, "A geometric active contour model without re-initialization for color images," *Image and Vision Computing*, Vol. 27, pp. 1411-1417, 2009.
- [18] C. Li, C. Xu, C. Gui, and M.D. Fox, "Level set evolution without re-initialization: A new variational formulation," *Proceedings of the IEEE Computer Society Conference on Computer Vision and Pattern Recognition*, Vol. 1, pp. 430-436, 2005.
- [19] C. Li, C. Xu, C. Gui, and M.D. Fox, "Distance regularized level set evolution and its application to image segmentation," *IEEE Transactions on Image Processing*, Vol. 19, pp. 3243-3254, 2010.
- [20] N.T.L. Anh, H.R. Park, L.T.K. Van, and G.S. Lee, "Object segmentation in color images using Distance Regularized Level Set," *KSII The first International Conference on Internet (ICONI)*, 2011.
- [21] N.T.L. Anh, Y.C. Kim, and G.S. Lee, "Morphological Gradient Applied to New Active Contour Model for Color Image Segmentation," *Proceedings of the 6th International Conference on Ubiquitous Information Management and Communication (ICUIMC)*, 2012.
- [22] Q.Z. Ge, L. Qiong, Z.C. Ling, X.X. Hui, and G. Zhang, "Stochastic motion and the level set method in semi-automatic building detection," *The International Archives of the Photogrammetry, Remote Sensing, and Spatial Information Sciences*, Vol. 37, pp. 431-434, 2008.
- [23] Y.N. Law, H.K. Lee, and A.M. Yip, "A Multiresolution Stochastic Level Set Method for Mumford-Shah Image Segmentation," *Image Rochester NY*, Vol. 17, pp. 2289-2300, 2008.
- [24] N. El-Zehiry and A. Elmaghraby, "A graph cut based active contour without edges with relaxed homogeneity constraint," *The 19th International Conference on Pattern Recognition*, pp. 1-4, 2008.
- [25] N. Xu, R. Bansal, and N. Ahuja, "Object segmentation using graph cuts based active contours," *Journal of Computer Vision and Image Understanding*, Vol. 107, pp. 210-224, 2007.
- [26] P. Ghosh, M. Mitchell, and J. Gold, "LSGA: combining level-sets and genetic algorithms for segmentation," *Evolutionary Intelligence*, pp. 1-11, 2010.
- [27] B. Sumengen and B.S. Manjunath, "Graph Partitioning Active Contours (GPAC) for Image Segmentation," *IEEE Transactions on Pattern Analysis and Machine Intelligence*, Vol. 28, pp. 509-521, 2006.
- [28] [http://vision.ece.ucsb.edu/~lbertelli/soft\\_GPAC.html](http://vision.ece.ucsb.edu/~lbertelli/soft_GPAC.html)
- [29] M.H. Siddiqi, S.Y. Lee, and Y.K. Lee, "Object Segmentation by Comparison of Active Contour Snake and Level Set in Biomedical Applications," *IEEE International Conference on Bioinformatics and Biomedicine*, pp. 414-417, 2011.
- [30] Y. Qiao and N. Minematsu, "f-divergence is a generalized invariant measure between distributions," *Proceedings of INTERSPEECH*, pp.1349-1352, 2008.
- [31] O. Michailovich, Y. Rathi, and A. Tannenbaum, "Image segmentation using active contours driven by the Bhattacharyya Gradient Flow," *IEEE Transactions on Image Processing*, Vol. 16(11), pp. 2787-2801, 2007.
- [32] T. Kailath, "The Divergence and Bhattacharyya Distance Measures in Signal Selection," *IEEE Transactions on Communication Technology*, Vol. 15, pp. 52-60, 1967.
- [33] R. Achanta, S. Hemami, F. Estrada, and S. Susstrunk, "Frequency-tuned salient region detection," *IEEE International Conference on Computer Vision and Pattern Recognition*, 2009.
- [34] <http://www.eecs.berkeley.edu/Research/Projects/CS/vision/grouping/resources.html>
- [35] [http://research.microsoft.com/vision/cambridge/recognition/MSR\\_C\\_ObjCategImageDatabase\\_v1.zip](http://research.microsoft.com/vision/cambridge/recognition/MSR_C_ObjCategImageDatabase_v1.zip)
- [36] [http://research.microsoft.com/vision/cambridge/recognition/MSR\\_C\\_ObjCategImageDatabase\\_v2.zip](http://research.microsoft.com/vision/cambridge/recognition/MSR_C_ObjCategImageDatabase_v2.zip)
- [37] F. Meyer, "Un algorithme optimal de partage des eaux," *8ième congress RFIA, Lyon-Villeurbanne*, pp. 847-857, 1991.
- [38] C. Rother, V. Kolmogorov, and A. Blake, "GrabCut – Interactive Foreground Extraction using Iterated Graph Cuts," *Proceeding of SIGGRAPH '04 ACM*, pp. 309-314, 2004.
- [39] A.K. Mishra, Y. Aloimonos, L.F. Cheong, and A.A. Kassim, "Active Visual Segmentation," *IEEE Transactions on Pattern Analysis and Machine Intelligence*, Vol. 34, No. 4, pp. 639-653, 2012.
- [40] H. Wang, M. Liu, and W.L. Ma, "Color Image Segmentation based on a New Geometric Active Contour Model," *IEEE International Conference on Machine Vision and Human-machine Interface*, pp. 6-9, 2010.
- [41] T.F. Chan, B.Y. Sandberg, and L.A. Vese, "Active Contours without Edges for Vector-valued Images," *Journal of Visual Communication and Image Representation*, Vol. 11, pp. 130-141, 2000.



**Nguyen Tran Lan Anh** received her M.S. degree in Computer Science from Chonnam National University, Republic of Korea in August, 2012. She is currently a lecturer at the Faculty of Mathematics and Computer Sciences at the University of Science, VNU-HCMC, Vietnam. Her research interests are multimedia and image processing, computer vision, and mobile

applications.



**Guesang Lee** received his B.S. degree in Electrical Engineering and M.S. degree in Computer Engineering from Seoul National University in 1980 and 1982, respectively. He received his Ph.D. degree in Computer Science from Pennsylvania State University in 1991. He is currently a professor of the Department of Electronics and Computer Engineering in Chonnam National University, Republic of Korea. His research interests are mainly in the field of image processing, computer vision and video technology.